Validation of a Tuning Method for Haptic Shared Control Using Neuromuscular System Analysis

Conference Paper · October 2014

DOI: 10.1109/SMC.2014.6974128

4 authors:

Emmanuel Sunil
Netherlands Aerospace Centre
38 PUBLICATIONS **566** CITATIONS
SEE PROFILE

Jan Smisek
Transcelestial Technologies
27 PUBLICATIONS **805** CITATIONS
SEE PROFILE

Marinus M. Van Paassen
Delft University of Technology
490 PUBLICATIONS **6,819** CITATIONS
SEE PROFILE

Max Mulder
Delft University of Technology
585 PUBLICATIONS **7,569** CITATIONS
SEE PROFILE

Validation of a Tuning Method for Haptic Shared Control Using Neuromuscular System Analysis

Emmanuel Sunil, Jan Smisek, Marinus M. van Paassen and Max Mulder

***Abstract*—This research investigates a neuromuscular analysis based tuning procedure for haptic shared control systems that has been hypothesized to improve subjective operator workload when compared to heuristic tuning methods. Here, the tuning procedure takes into consideration the response of the neuromuscular system to haptic cues. Human arm stiffness, the neuromuscular property of concern, can be changed by modulating reflex strength. The 'relax task' setting of the neuromuscular system, for which reflexes are minimized, is chosen as the design point for tuning haptic cues as it is hypothesized to lead to the lowest workload. A simulated haptic collision avoidance system for unmanned aircraft teleoperation is used as a platform to experimentally validate the tuning method. The results show that the novel tuning procedure, particularly for relax task tuning, substantially improves workload and situational awareness over conditions that ignores the neuromuscular system. Additionally, over-tuning, which frequently occurs for heuristic methods, leads to worse user acceptance than a condition without haptic support.**

***Index Terms*—Tuning haptic shared control, neuromuscular admittance, haptic human-machine interface, force-feedback support system, human-centered design, unmanned aerial vehicle (UAV), collision avoidance.**

I. Introduction

In Haptic Shared Control (HSC) systems, a human operator and an automatic controller share control of a process by simultaneously exerting guidance forces/moments on a common Control Interface (CI). The resulting position of the CI is the only input to the controlled process. This distinct property of HSC ensures that the human operator is continuously informed about the intentions of the automation, allowing the operator to actively take part in the decision making process through intuitive haptic interactions [1]. For these reasons, HSC has been proposed as a control paradigm that has the potential to overcome some of the human-machine interaction issues frequently associated with pure manual and automatic control systems [1], [2].

Numerous examples of HSC can be found in literature with applications ranging from telerobotics to vehicular control [2], [3]. An interesting application of HSC in aviation is the use of haptic feedback to improve the safety of Unmanned Aerial Vehicles (UAVs). This interface, termed the Haptic Collision Avoidance System (HCAS), augments visual feedback from onboard cameras with haptic guidance moments applied on a control-loaded side-stick to help teleoperators in steering a UAV away from obstacles [4]. Experiments have indicated that the HCAS significantly improved the safety of teleoperation, but at the cost of increased workload [4], [5]. Other implementations of HSC have also reported similar issues [2].

These early examples of HSC used heuristic tuning of haptic moments with the aim of optimizing overall system performance. Recent research has shown that heuristic tuning can result in disagreements between the human operator and the automation on a haptic level [6]. The difficulty with heuristic tuning has been attributed to the large adaptation range of the Neuromuscular System (NMS), which is able to adapt its properties such that performance and overall system stability are satisfactory, regardless of the specific tuning used. However, adaptations to 'non-optimal' settings of the NMS, as is often the case with heuristic tuning methods, can cause haptic cues to be perceived as 'too strong', resulting in increased user discomfort and workload over time [7].

The goal of this research is to experimentally validate a novel neuromuscular analysis based tuning procedure for HSC. Here, haptic cues are tuned to match a so called 'design neuromuscular setting' where properties of the NMS are known and are desirable for the control task under consideration [7], [8]. This method may enable the NMS to adapt to a tuning setting that is based on its own properties, thus possibly reducing conflicts and improving the haptic interaction between the human operator and the automation. The aforementioned HCAS is used as a platform to experimentally test the new method, using NMS measurements taken by Smisek et al. [9].

The paper begins with descriptions of the HCAS and the neuromuscular analysis based tuning procedure in Section II and Section III respectively. This is followed in Section IV with the design and results of the experiment. Finally, the main conclusions are summarized in Section V.

II. Haptic Collision Avoidance System

This study uses the HCAS as the framework for testing a new HSC tuning procedure. Therefore the functionality of the HCAS is briefly outlined in this section.

A. System Architecture

A block diagram schematic of the HCAS is depicted in Fig. 1. Here it can be seen that the outer visual feedback loop of the UAV teleoperator is complemented with an inner haptic feedback loop originating from an automatic controller. Like other HSC systems, the automatic controller can be divided into two separate components or 'mappings' [6]. The first mapping, which replicates the visual/cognitive control task of the teleoperator, is performed by a so called 'Parametric Risk Field' (PRF). The PRF, a type of Artificial Force Field

The authors are with the Control and Simulation division, Faculty of Aerospace Engineering, Delft University of Technology, Kluyverweg 1, 2629HS Delft, The Netherlands. Email: e.sunil@tudelft.nl

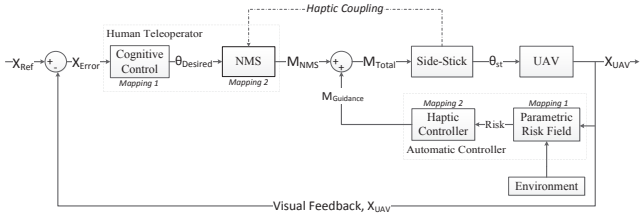

Fig. 1. Haptic collision avoidance system (HCAS) architecture, based on the principles of haptic shared control (HSC). A 'haptic-coupling' exists between the neuromuscular system (NMS) and the side-stick, as long as physical contact is maintained.

(AFF), scans the environment for obstacles and computes the corresponding risk of collision [10]. This risk is converted to a haptic guidance moment, $M_{Guidance}$, by the 'haptic controller'. The function of the haptic controller is similar to that of the NMS and it constitutes the second mapping of the automation. The tuning of this second mapping is the focus of the current research.

The haptic guidance moment, $M_{Guidance}$, and the moment generated by the teleoperator NMS, M_{NMS}, act together on the side-stick, and its resulting position, θ_{st}, dictates the sole steering command issued to the UAV. In terms of collision avoidance assistance, the magnitude of $M_{Guidance}$ indicates the severity of a potential collision, whilst its direction suggests a collision avoidance steering maneuver that the teleoperator can follow to safely navigate around obstacles.

B. Division of Control Authority

The division of control authority between the human operator and the automation is influenced mainly by the tuning of the haptic controller [1]. To promote safe system operation in the event of automation failures, the human operator must always have the ability to overrule the automation. Consequently, the haptic controller must be designed to ensure that $M_{Guidance}$ is always less than M_{NMS}.

The primary objective for early implementations of the HCAS (and other forms of HSC) was to improve system performance and safety over pure manual control. To realize this goal, the haptic controller was typically tuned using heuristic methods, often resulting in very strong haptic guidance moments. While 'over-tuning' haptic cues improved safety, it also biased control authority towards the automation [5]. As a result, many subjects complained that haptic moments felt too difficult to override, causing high subjective operator workload [5]. To improve user acceptance of HSC systems, it is necessary to tune haptic cues such that workload is reduced without sacrificing system safety, nor human control authority over the automation.

III. Tuning Haptic Feedback

This section introduces a new 'human-centered' tuning approach for haptic cues that is based on properties and measurements of the NMS. First, neuromuscular properties relevant to the tuning approach are presented. Subsequently, the theoretical rationale behind the approach is explained.

A. Properties of the Human Neuromuscular System

With respect to the tuning of the haptic controller, an important dynamic property of the NMS is its admittance to external (haptic) forces/moments. Admittance is formally defined as the "causal relationship between moment (input) and hand position (output)" [3]. It can be "thought of as a measure of the displacement that a moment causes" [3]. In practical terms, admittance is equal to the 'inverse stiffness' of the NMS (at low external moment/excitation frequencies i.e., ≤ 2 [Hz]) [3]. Additionally, empirical evidence has found that admittance is dependent on the magnitude and direction of manual control (moment) inputs applied on the CI [8], [9].

The NMS is highly adaptive as admittance can be varied over a wide range of values through two physiological mechanisms: fast subconscious spinal reflexes and muscle pair co-contraction [3]. Using these two mechanisms, humans can be instructed to respond to external moments in three distinct ways known in literature as the force (FT), relax (RT) and position (PT) tasks [3], see Table I.

B. Neuromuscular Admittance Based Tuning Method

Haptic guidance moments applied on the CI are transmitted to the human operator via his/her NMS. Therefore it is necessary to include the response of the NMS to haptic cues when tuning the haptic controller [6], [7]. Effectively, this approach uses the combined stiffness (i.e., inverse admittance) of the NMS and the CI to compute haptic cues, see Fig. 2. For the HCAS, the resulting tuning law can be expressed as:

$$\begin{bmatrix} M_{Guidance_X} \\ M_{Guidance_Y} \end{bmatrix} = \underbrace{[\mathbf{K_{NMS}}(\theta_{\mathbf{st}}) + \mathbf{K_{st}}]}_{combined\ system\ stiffness} \begin{bmatrix} Risk_X \\ Risk_Y \end{bmatrix} \quad (1)$$

Here $\mathbf{K_{NMS}}$ is the stiffness of the NMS and $\mathbf{K_{st}}$ is the stiffness of the side-stick CI. The 'risk vector' in eq. 1 represents the output of the PRF i.e, the first mapping of the automation, see Fig. 1. Note that the tuning law accounts for the dependence of $\mathbf{K_{NMS}}$ on the magnitude and direction of manual control inputs applied on the side-stick, $\theta_{\mathbf{st}}$. Thus $\mathbf{K_{NMS}}$ and $\mathbf{K_{st}}$ are defined separately along the longitudinal (X) and lateral (Y) hand/stick axes:

$$\mathbf{K_{NMS}}(\theta_{\mathbf{st}}) = \begin{bmatrix} K_{NMS_X}(\theta_{\mathbf{st}}) & 0 \\ 0 & K_{NMS_Y}(\theta_{\mathbf{st}}) \end{bmatrix} \quad (2)$$

$$\mathbf{K_{st}} = \begin{bmatrix} K_{st_X} & 0 \\ 0 & K_{st_Y} \end{bmatrix} \quad (3)$$

TABLE I
Description of the three neuromuscular task instructions

Task	Admittance	Description
Force Task (FT)	High	Yield to haptic moments and the motion of control interface
Relax Task (RT)	Medium	Do not react to haptic moments and follow motion of control interface
Position Task (PT)	Low	Resist haptic moments and maintain position of control interface

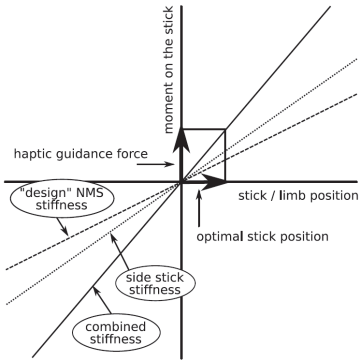

Fig. 2. Rationale behind the novel tuning procedure [9]. Here it is proposed that a haptic guidance moment corresponding to the combined system stiffness i.e., stiffness of stick + design neuromuscular stiffness, has to be provided by the haptic controller to obtain the desired, or optimal, stick deflection.

To implement the tuning method described above, an appropriate value for K_{NMS} has to be selected. Three possible design options correspond to the stiffness/admittance profiles of FT, RT and PT neuromuscular task instructions, see Table I.

In this study, the relax task (RT) stiffness is selected as the design point for tuning the haptic controller. This is because reflexes are naturally suppressed when performing the RT and the properties of the NMS are mainly dependent on its intrinsic stiffness and damping characteristics [3]. Consequently, the RT leads to the lowest physical activity of the three neuromuscular task instructions, thus the selection of the RT is closely aligned with the goal of reducing workload for HSC. Using RT admittance measurements taken by Smisek et al. [9], the tuning method can be tested in the context of the HCAS.

IV. Human-In-The-Loop-Experiment

To validate the novel tuning method described in Section III-B, a human-in-the-loop experiment that simulated UAV teleoperation was conducted using a repeated-measures design. This section presents the design and results of the experiment.

A. Experiment Design

1) Subjects and Task Instruction: Twelve right-handed male subjects, with an average age of 23.4 years (σ = 0.7 years), took part in the experiment. Subject consent was obtained prior to the experiment and no monetary compensation was offered.

During the experiment, subjects were required to perform a UAV remote sensing task in an obstacle laden urban environment. Subjects were instructed, in order of priority, to avoid collisions, fly as closely as possible through the center of waypoints (represented as smoke plumes), and to perform the task as quickly as possible. To improve experiment realism, each collision resulted in a twenty second time penalty during which the experiment was paused.

2) Apparatus: A fixed-base flight simulator was used to perform the experiment, see Fig. 3. Visual cues of the surroundings were projected on a wall in front of the subject, originating from a simulated onboard camera fixed to the longitudinal axis of the UAV. Additionally, a navigation display with a 'top-down' view was provided.

An electro-hydraulic side-stick was used for manual control of the UAV and to supply haptic collision avoidance moments. Second order dynamics with an inertia $I_{st} = 0.02$ [kgm^2], a damping coefficient $B_{st} = 0.2$ [Nms/rad], and a spring constant $K_{st} = 2.0$ [Nm/rad] were simulated on both stick axes. The length of the side-stick, from the axis of rotation to the middle of the hand, was 0.09 [m].

The UAV was modeled as an 'easy-to-fly' helicopter with a rotor diameter of 3.0 [m] [4]. Longitudinal side-stick inputs were mapped to velocity commands (max 5.0 [m/s]), whereas lateral inputs were mapped to yaw rate commands (max 0.32 [rad/s]). The UAV altitude was kept constant by an autopilot.

3) Haptic Controller Implementation: The haptic controller was implemented using the average RT admittance of ten subjects measured by Smisek et al. [9], at a measurement/excitation signal frequency of 0.5 [Hz]. In that study, RT admittance was measured in the presence of manual control inputs on a two degree of freedom CI. As a result, the compiled data is more representative of neuromuscular dynamics during real-life control tasks when compared to previous admittance measurement techniques (where identification was usually performed without voluntary manual control inputs). For more details on the admittance identification procedure, the reader is referred to [9].

To study the dependence of admittance on the magnitude and direction of manual control inputs, Smisek et al. [9] measured admittance for thirteen different conditions, see Fig. 4. This dependence is taken into account when tuning the haptic controller by using nearest neighbor interpolation

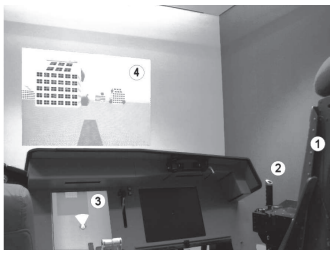

Fig. 3. Fixed-base flight simulator with aircraft chair (1), hydraulic side-stick (2), navigation display (3) and onboard camera view (4)

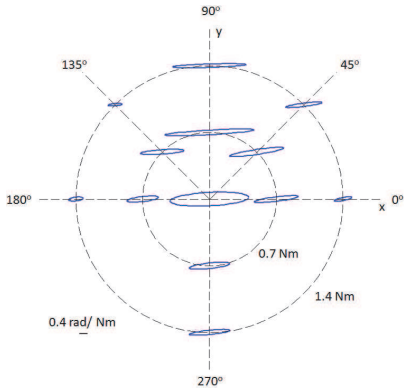

Fig. 4. RT admittance identification results for one subject ($f = 0.5$ [Hz]), for the thirteen manual control input conditions used by Smisek et al. [9]. The length of the major and the minor axes of each ellipse indicates the admittance along these two directions for all measurement conditions.

(of the instantaneous teleoperator manual control input's magnitude and direction) to determine the nearest measurement condition visualized in Fig. 4. Subsequently, the measured NMS admittance/stiffness values for the 'nearest condition' (K_{NMS_X} and K_{NMS_Y}) are used to compute appropriate haptic cues using eq. 1. It is hoped that this dynamic tuning approach will allow the haptic controller to better anticipate the real time stiffness of the NMS, and consequently improve the teleoperator's appreciation of haptic cues.

4) Independent Variables: Two categories of independent variables were defined for the experiment. The first category was concerned with the tuning profile (TP) of the haptic controller (HC). A total of four TPs were tested, resulting in the four experiment conditions listed in Table II. Here, UT and OT controllers represent TPs that are half and twice as strong as RT tuning, respectively. These two TPs were defined to study the sensitivity of the novel tuning procedure.

The second independent variable was obstacle (OB) and six obstacles, displayed as buildings of different shapes, made up the virtual environment of the remote sensing task, see Fig. 5. Each obstacle was designed to evoke different control behavior. Obstacles were arranged randomly to create three measurement and three training trajectories to reduce boredom and learning effects.

5) Dependent Measures: The dependent measures used to compare different TPs are described in Table III.

6) Procedure: The experiment began with a training session to allow subjects to practice controlling the UAV with the aid of haptic cues. Afterward, subjects flew four measurement runs for each TP. Experiment conditions were randomized and subjects had no prior knowledge of the conditions performed. At the end of each condition, subjective workload (using NASA TLX), situational awareness (SA) and haptic feedback acceptance (HA) were measured using questionnaires. The total duration of the experiment, including training, breaks and the pre-experiment briefing was 2 hours.

B. Experiment Results and Discussion

All objective dependent measures, except subjective questionnaires, were computed per obstacle to take into account the different order of obstacles in each trajectory. Subsequently, the effects of the independent variables (TP and OB) on the dependent variables were analyzed using statistical methods. Interval/ratio dependent measures were studied using full-factorial repeated-measures ANOVA (Analysis of Variance),

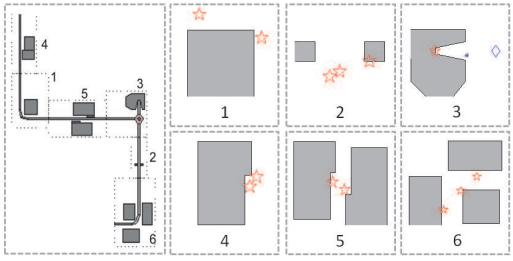

Fig. 5. An example trajectory composed of six obstacles arranged randomly. Waypoints are pictured as red stars. Trajectories took approximately two minutes and thirty seconds to complete (when flown without collisions).

TABLE II
EXPERIMENT CONDITIONS

	Symbol	Description
1	NHF	No haptic feedback / pure manual control
2	RT	HC tuned based on relax task admittance data collected by Smisek et. al [9] ($f_{dist} = 0.5Hz$)
3	UT	HC under-tuned relative to RT ($UT = 0.5RT$)
4	OT	HC over-tuned relative to RT ($OT = 2RT$)

TABLE III
EXPERIMENT DEPENDENT MEASURES

Measure	Symbol	Description
Safety	$n_{collisions}$	Number of collisions [-]
Performance	$\overline{V}$	Mean velocity [m/s]
	d_{wp}	Min distance to waypoints [m]
Control Activity	$\sigma_{\dot{\delta}\,st}$	Standard deviation of stick rate [rad/s]
Haptic Activity	$\sigma_{M_{Guidance}}$	Standard deviation of haptic guidance moment [Nm]
Subjective	NASA TLX	Workload assessment survey
	SA	Situational awareness survey
	HA	Haptic feedback acceptance survey

with pairwise Bonferroni corrected comparisons used as post-hoc tests. To comply with ANOVA assumptions, Greenhouse-Geisser corrections were applied to the degrees of freedom for non-spherical data. Ordinal dependent measures ($n_{collisions}$ and subjective questionnaires) were inspected using the Friedman test with Wilcoxon signed-rank tests used for post-hoc analysis (also with Bonferroni corrections).

1) Safety: Fig. 6a shows that the number of collisions, $n_{collisions}$, decreased with increasing strength of the haptic controller, and was the lowest for the OT condition. However, the Friedman test revealed only a marginally significant effect of TP on $n_{collisions}$ (TP: $\chi^2(3) = 7.48$, $p = 0.058$). This statistical artifact may be due to the very few collisions that occurred for the entire experiment. In fact, total $n_{collisions}$ for all conditions was found to be significantly lower than previous experiments with the HCAS [4], [5]. This could be a result of the twenty second collision penalty applied in this work that encouraged subjects to fly as safely as possible. The Friedman test did show a highly significant effect of OB on $n_{collisions}$, (OB: $\chi^2(5) = 17.31$, $p \leq 0.01$). Obstacle 5, which resulted in the highest number of collisions, was also reported by subjects to be the most difficult, see Fig. 6b.

2) Performance: The mean velocity of the UAV, $\overline{V}$, is shown in Fig. 6c. Here it can be seen that for a particular obstacle, $\overline{V}$ was relatively constant for all haptic controllers, resulting in no statistical significance of TP on $\overline{V}$. On the other hand, $\overline{V}$ varied substantially with OB, causing a highly significant effect (OB: $F_{2.39,26.29} = 107.16, p \leq 0.01$). When comparing Fig. 6c with Fig. 6b, it can be seen that velocity tends to be lower for obstacles with a higher number of collisions. This indicates that subjects decreased UAV velocity in an attempt to follow the primary task instruction of avoiding collisions, particularly for difficult obstacles.

Similar to $\overline{V}$, the minimum distance to waypoints, d_{wp}, was

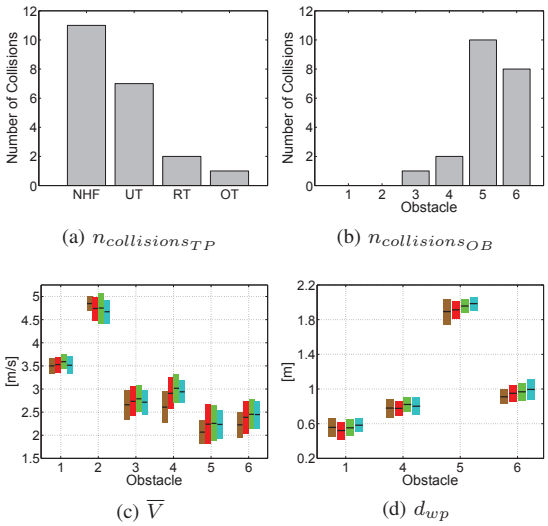

(a) $n_{collisions_{TP}}$ (b) $n_{collisions_{OB}}$

(c) $\overline{V}$ (d) d_{wp}

Fig. 6. Means and 95% confidence intervals of safety and performance related dependent variables. Obstacles 2 and 3 did not have smoke plumes serving as waypoints. NHF(brown), UT(red), RT(green) and OT(cyan).

not influenced by TP, but affected significantly by OB (OB: $F_{3,33} = 296.79, p \leq 0.01$), see Fig. 6d. Moreover, it can be seen that d_{wp} followed the same trend as $n_{collisions_{OB}}$ and obstacles with more collisions had higher d_{wp}. This provides additional evidence that subjects employed a conservative control strategy when tackling difficult obstacles.

Based on these results, it is clear that TP had no measurable effect on performance. This may be due to subjects adapting their control strategies to ensure that task instructions are followed with similar performance for all TPs. This suggests that it is difficult to select an appropriate tuning setting using performance metrics alone.

3) Control Activity: The standard deviation of the longitudinal side-stick deflection rate, $\sigma_{\dot{\delta}st_X}$, is pictured in Fig. 7a. For all obstacles, $\sigma_{\dot{\delta}st_X}$ was the smallest for NHF and the largest for OT, a highly significant effect (TP: $F_{1.33,14.59} = 19.56, p \leq 0.01$). Fig. 7a also shows that $\sigma_{\dot{\delta}st_X}$ was significantly lower for obstacle 2 (OB: $F_{1.93,21.27} = 42.80, p \leq 0.01$).

In the lateral direction, $\sigma_{\dot{\delta}st_Y}$ was also the highest for the OT controller (TP: $F_{3,33} = 17.57, p \leq 0.01$), see Fig. 7b. Similar to the longitudinal direction, post-hoc tests revealed no significant differences between UT and RT for $\sigma_{\dot{\delta}st_Y}$. As no turns are necessary to complete obstacle 2, this obstacle resulted in the lowest $\sigma_{\dot{\delta}st_Y}$, a highly significant effect (OB: $F_{1.93,21.27} = 25.95, p \leq 0.01$).

For most cases, control activity was higher in the lateral direction. This can be explained by the continuous corrective lateral stick inputs required to meet the secondary objective of flying through the center of waypoints.

4) Haptic Activity: The standard deviation of the longitudinal haptic guidance moment, $\sigma_{M_{Guidance_X}}$, shown in Fig. 7c, increased with increasing strength of the haptic controller, an effect of high statistical significance (TP: $F_{1.35,14.87} = 75.88, p \leq 0.01$). Post-hoc tests showed highly significant differences between all three haptic controllers ($p \leq 0.01$). In terms of OB, variations increased from obstacle 1 to 6, a statistically significant effect (OB: $F_{2.66,29.24} = 6.50, p \leq 0.05$).

Variations of the lateral haptic guidance moment, $\sigma_{M_{Guidance_Y}}$, are much greater for obstacles 4-6 when compared to obstacles 1-3, a highly significant effect (OB: $F_{2,22} = 9.57, p \leq 0.01$), see Fig 7d. Unsurprisingly, OT produced the largest $\sigma_{M_{Guidance_X}}$ for all obstacles (TP: $F_{2,22} = 9.57, p \leq 0.01$). Post-hoc tests showed no significant differences between UT and RT controllers.

It is interesting to note that haptic activity decreased in the lateral direction, while control activity was found to be higher laterally. Due to the feedback architecture of the HCAS, greater lateral stick motion combined with a decrease in lateral haptic activity implies that subjects were more willing to follow lateral haptic cues. This result may be closely related to the limited lateral visual cues provided, forcing subjects to rely on lateral haptic guidance moments for collision avoidance.

5) Subjective Questionnaires: Fig. 8a displays overall workload, or Z-score, computed using the NASA TLX subjective questionnaire. Here a lower subjective rating symbolizes lower workload. A Friedman test showed that there was a highly significant effect of TP on overall workload (TLX: $\chi^2(3) = 18.10$, $p \leq 0.01$). Post-hoc analysis using the Wilcoxon test revealed that significant differences were caused by the extreme conditions, NHF and OT, which had the highest workload levels. However, no substantial differences were recorded between UT and RT, and these two controllers led to the lowest measured workload. These results suggest that including the response of the NMS when computing haptic cues, as for RT, can *decrease* overall subjective workload with respect to NHF.

The six workload sources of the NASA TLX are pictured in Figs. 8b to 8g. The reduction of overall workload for UT/RT compared to NHF can be traced back to a reduction of mental load (ML) and effort (EF) for these two haptic controllers

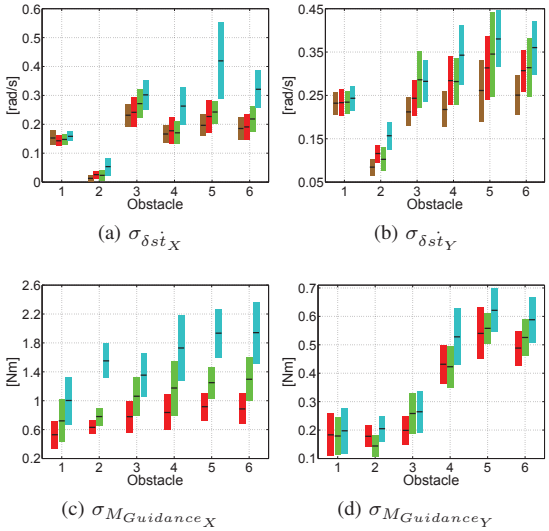

(a) $\sigma_{\dot{\delta}st_X}$ (b) $\sigma_{\dot{\delta}st_Y}$

(c) $\sigma_{M_{Guidance_X}}$ (d) $\sigma_{M_{Guidance_Y}}$

Fig. 7. Means and 95% confidence intervals of control and haptic activity related dependent variables. NHF(brown), UT(red), RT(green) and OT(cyan).

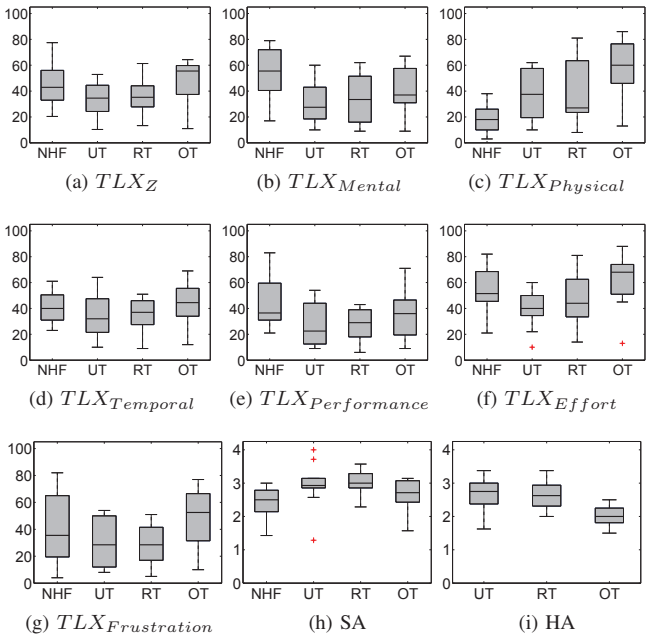

(a) TLX_Z (b) TLX_{Mental} (c) $TLX_{Physical}$

(d) $TLX_{Temporal}$ (e) $TLX_{Performance}$ (f) TLX_{Effort}

(g) $TLX_{Frustration}$ (h) SA (i) HA

Fig. 8. Medians and interquartile ranges of the subjective dependent variables, with outliers (+). SA stands for Situational Awareness and HA for Haptic Acceptance.

(ML: $\chi^2(3) = 16.20$, $p \leq 0.01$; EF: $\chi^2(3) = 15.91$, $p \leq 0.01$). This is in sharp contrast to earlier research where haptic cues contributed negatively towards mental load and effort [5]. However, physical load (PL) continued to be higher for the novel tuning method, and increased with the strength of the haptic controller, a highly significant effect (PL: $\chi^2(3) = 25.23$, $p \leq 0.01$). Despite improvements in performance, frustration and temporal load for UT/RT, TP did not result in statistically relevant effects for these measures.

Box plots for subjective situational awareness (SA) and haptic feedback acceptance (HA) are given in Figs. 8h and 8i. For these two indicators, higher subjective ratings imply better SA and HA. A Friedman test showed a highly significant effect of TP on SA, with the highest and lowest median SA recorded for RT and NHF respectively (SA: $\chi^2(3) = 11.58$, $p \leq 0.01$). A similar trend was found for HA, with the highest acceptance for RT and the lowest for OT, a significant effect (HA: $\chi^2(2) = 8.21$, $p \leq 0.05$).

The results of the three subjective questionnaires indicate that acceptance of haptic cues increased for UT and RT haptic controllers. Over-tuning the controller was found to be more detrimental than providing no haptic support. This supports the notion that heuristic tuning can adversely impact user acceptance of HSC systems.

V. Conclusion

The primary objective of this study is to validate a systematic tuning approach for haptic shared control (HSC) systems that uses neuromuscular admittance measurements of the human arm. The results of an experiment conducted to validate the novel tuning approach showed that subjective workload and situational awareness improved significantly for the under-tuned and the relax task tuned haptic controllers when compared to pure manual control. Additionally, the results suggested that over-tuning the haptic controller, as is usually the case for heuristic tuning methods, yields lower user acceptance than the condition with no haptic support. These results strongly indicate that including neuromuscular response in the haptic controller tuning procedure improves overall user acceptance the system.

For most dependent variables, no statistical differences were found between the under and the relax task tuned controllers. This result reveals that the design space available for selecting an appropriate tuning profile is larger than expected: a range of values between the admittance characteristics of the under and relax task tuned controllers can improve user acceptance relative to manual control. This conclusion also implies that a selection between these two tuning options depends on the specific application of haptic cues and the experience of the intended user with haptic interfaces. For applications involving inexperienced users (e.g. car driving), under-tuning the haptic controller (up to half the strength of the relax task controller) is an acceptable option as a tendency was found in this research for subjects to prefer the smallest haptic assistance necessary to complete a given task. For professional settings, as for UAV teleoperation, relax task tuning presents a better middle ground between user acceptance and safety.

Due to the limited lateral visual cues supplied during the experiment, subjects had a greater appreciation for lateral haptic cues. However in the longitudinal direction, differences between haptic and visual cues provided led to 'goal' related conflicts. These conflicts need to be addressed in the future to further improve user acceptance of HSC systems.

References

[1] D. A. Abbink, M. Mulder, and E. R. Boer, "Haptic shared control: smoothly shifting control authority?" *Cognition, Technology & Work*, vol. 14, no. 1, pp. 19–28, Mar. 2012.

[2] P. G. Griffiths and R. B. Gillespie, "Sharing control between humans and automation using haptic interface:primary and secondary task performance benefits," *Human Factors: The Journal of the Human Factors and Ergonomics Society*, vol. 47, no. 3, pp. 574–590, Sep. 2005.

[3] D. A. Abbink, "Neuromuscular analysis of haptic gas pedal feedback during car following," PhD, Delft University of Technology, Delft, 2006.

[4] T. M. Lam, "Haptic interface for UAV teleoperation," Ph.D. dissertation, Delft University of Technology, Delft, May 2009.

[5] T. M. Lam, M. Mulder, and M. M. van Paassen, "Haptic interface for UAV collision avoidance," *The International Journal of Aviation Psychology*, vol. 17, no. 2, pp. 167–195, 2007.

[6] D. A. Abbink, D. Cleij, M. Mulder, and M. M. Van Paassen, "The importance of including knowledge of neuromuscular behaviour in haptic shared control," in *2012 IEEE International Conference on Systems, Man, and Cybernetics (SMC)*, Oct. 2012, pp. 3350 –3355.

[7] D. A. Abbink and M. Mulder, "Neuromuscular analysis as a guideline in designing shared control," *Advances in Haptics*, vol. 109, 2010.

[8] J. Lasschuit, T. Lam, M. Mulder, M. M. Van Paassen, and D. Abbink, "Measuring and modeling neuromuscular system dynamics for haptic interface design," in *Proceeding of the AIAA Modeling and Simulation Technologies Conference and Exhibit*, Aug. 2008.

[9] J. Smisek, M. M. van Paassen, M. Mulder, and D. A. Abbink, "Neuromuscular analysis based tuning of haptic shared control assistant for UAV collision avoidance," in *IEEE World Haptics Confrence*, 2013.

[10] T. M. Lam, H. W. Boschloo, M. Mulder, and M. M. van Paassen, "Artificial force field for haptic feedback in UAV teleoperation," *IEEE Transactions on Systems, Man and Cybernetics, Part A: Systems and Humans*, vol. 39, no. 6, pp. 1316 – 1330, Nov. 2009.